Am J Cancer Res 2014;4(6):629-647
www.ajcr.us /ISSN:2156-6976/ajcr0001852

Original Article

Mahanine, a novel mitochondrial complex-III inhibitor induces G0/G1 arrest through redox alteration-mediated DNA damage response and regresses glioblastoma multiforme

Kaushik Bhattacharya[1*], Arup K Bag[1*], Rakshamani Tripathi[2], Suman K Samanta[1], Bikas C Pal[3], Chandrima Shaha[2], Chitra Mandal[1]

[1]*Cancer Biology and Inflammatory Disorder Division, Council of Scientific and Industrial Research (CSIR)-Indian Institute of Chemical Biology, 4, Raja S.C. Mullick Road, Jadavpur, Kolkata-700032, India;* [2]*Cell Death and Differentiation Research, National Institute of Immunology, New Delhi, India;* [3]*National Institute of Pharmaceutical Education and Research, Kolkata, India.* [*]*Equal contributors.*

Received August 12, 2014; Accepted September 30, 2014; Epub November 19, 2014; Published November 30, 2014

Abstract: The Electron transport chain (ETC) is responsible for oxidative phosphorylation-mediated mitochondrial respiration. Here we wanted to address the mahanine-induced targeted pathways in glioblastoma multiforme (GBM) in the context of G0/G1 phase arrest and redox alteration. We have demonstrated mahanine, as a novel mitochondrial complex-III inhibitor which induced G0/G1 phase arrest in GBM. This event was preceded by accumulation of intracellular ROS by the inhibition of mitochondrial ETC. The accumulated ROS induced DNA damage response (DDR), that mediated Chk1/Chk2 upregulation and activation which were essential factors for the G0/G1 arrest. NAC-mediated scavenging of ROS generation reduced the propensity of G0/G1 phase arrest in GBM cells by mahanine. Knockdown of Chk1/Chk2 also affected the cell cycle inhibitory potential of mahanine. During G0/G1 arrest, other hallmark proteins like, cyclin D1/cyclin D3, CDK4/CDK6 and CDC25A were also downregulated. The G0/G1 phase restriction property of mahanine was also established in *in vivo* mice model. Mahanine-induced complex-III inhibition triggered enhanced ROS in hypoxia responsible for higher G0/G1 arrest. Furthermore, we demonstrated that mahanine-treated G0/G1 arrested cells were less potent to form xenograft tumor *in vivo*. Additionally, they exhibited reduced ability to migrate and form intracellular tube-like structures. Moreover, they became susceptible to differentiate and astrocyte-like cells were generated from the epithelial lineage. Taken together, our results established that complex-III of ETC is one of the possible potential targets of mahanine. This nontoxic chemotherapeutic molecule enhanced ROS production, induced cell cycle arrest and thereafter regressed GBM without effecting normal astrocytes.

Keywords: G0/G1 arrest, mitochondrial ETC, ROS, DNA damage response, glioblastoma multiforme, mahanine

Introduction

Reactive oxygen species (ROS) is a combined form of both oxygen radicals (superoxide and hydroxyl) and some non-radical derivatives as hydrogen peroxide [1]. Electron transport chain (ETC) probably is the most important intracellular resource of ROS. In the eukaryotic organism, the location of the ETC is mainly in the mitochondria and endoplasmic reticulum. In the mitochondrial ETC, series of oxidation-reduction reactions occur between different reductants and oxidants by the flow of electrons and protons [1]. However, during the transfer of electrons, a few may leaked out and convert O_2 into highly reactive superoxide anion. It then triggers the damage to mitochondrial membrane potential and cell may undergo apoptosis [2]. Different mitochondrial ETC complex blockers trigger high amount of ROS and therefore promote cancer cell death [3, 4].

The cell cycle is a sequential series of actions by which an emergent cell duplicates all of its machinery and splits into two progenitor cells. Under normal condition, after division of the cells in the mitotic (M) phase, they enter into G1 and then G0 phase for proper development and maturation [5, 6]. Mature cells then go through S and G2 phases to complete the cycle. It is the

cyclin D family of proteins involved with CDK4/CDK6, responsible for early G1 regulation. Association of cyclin E with CDK2 is mainly responsible for the G1 to S transition [5-7]. DNA damage response (DDR) induces the activation of check point kinases (Chk1/Chk2) and thereby regulates G0/G1 arrest [8, 9]. CDC25A, an oncogenic phosphatase, is also responsible for CDK2 activity and hence regulate cell cycle progression [9].

GBM is the most common and highest grade of malignant primary brain tumor in humans and mainly originates in glial cells with highest mortality rate [10, 11]. Despite advances in clinical and surgical neuro-oncology, the diagnosis, prognosis and treatment remain poor. The overall survival rate for 1 year is only ~40%, although a combined radiotherapy and chemotherapy does result in some improvement (~46%) [12]. Structure of the blood brain barrier is degenerated in GBM [13]. Various oncogene-activating mutations and the repression or deletion of tumor-suppressor genes are frequently found and are involved in disease progression [11, 14, 15]. A large portion (30-35%) of patients is diagnosed with the particularly lethal oncogenic EGFRvIII mutation [16, 17].

Till today, there is an acute shortage of proper chemotherapeutic agents for GBM. The main agents are temozolomide, RTK inhibitors and the cetuximab. However they show poor success rate and high degree of toxicity [18, 19]. Drug-unresponsiveness is also a typical problem [19, 20]. Therefore, the introduction of new molecules having a low level of toxicity with improved efficacy is urgently required [21]. Mahanine, a carbazole alkaloid, induces Fas/FasL and mitochondrial activation-mediated apoptosis in leukemia both *in vitro* and *in vivo* with minimal toxicity to tissues [22, 23]. It also induces redox-alterations which destabilize Hsp90 chaperone activity, suggesting a specific role in pancreatic cancer [23, 24]. Anti-cancer activity in histiocytic lymphoma, promyelocytic leukemia and prostate cancer cells were also reported [25-28]. We have identified that mahanine triggered its cytotoxicity through C-7-OH and 9-NH functional groups and it is a DNA minor grove-binding agent [29]. Also mahanine-induced ROS accumulate a tumor suppressor protein (PTEN) in nucleus and activates p53/p73-mediated apoptosis alone and in synergy with 5-flurouracil in colorectal carcinoma cells [30]. Additionally, it reduces 5-8 fold cisplatin concentration when used in adjunct with mahanine for the apoptosis of cervical cancer [26].

We have earlier established that mahanine modulates redox potential in the cancer cells, here we mainly addressed the major targeted-pathway responsible for the cell cycle regulation, mediated by redox manipulation in mahanine-treated GBM cells. As identification of target molecule enhances the value of chemotherapeutic agents, we have taken this approach to identify the probable major target for mahanine. Our results suggested that mitochondrial complex-III is one of the potential targets of mahanine and its inhibition mediated accumulation of ROS, an essential factor for DDR. This DDR mediated Chk1/Chk2 upregulation and their activation trigger the G0/G1 phase arrest in mahanine-treated GBM cells both *in vitro* and *in vivo* systems and reverted different oncogenic properties of cancer cells/tissues. Oxidative manipulations by mahanine also overcome hypoxia-induced probable drug resistance. Taken together, our results suggest that mahanine is a potential new candidate for GBM.

Materials and methods

Reagents

The primary antibodies of p-Chk1 (Ser 317, Ser 296), Chk1, p-Chk2 (Thr 68, Ser 516, Ser 19), Chk2, CDC25A, cyclin D1, cyclin D3, CDK4, CDK6, cyclin E, CDK2, GFAP, β-actin, HIF1α and HRP-conjugated secondary antibodies were purchased from Cell Signaling Technology (USA). Flow cytometry compatible FITC-conjugated anti-rabbit IgG (H + L), FCS, H_2DCFDA, mitotracker deep red, Trypsin-EDTA and IMDM cell culture medium were purchased from Invitrogen (USA). esiRNAs, N-TER nanoparticle driven transfection system, antibiotic–antimycotic, PI (Propidium Iodide), NAC, MTT, molecular grade BSA, Tween-20, Tris-HCl, EGTA, mannitol, sucrose, HEPES, KOH, KCl, KH_2PO_4, $MgCl_2$, MOPS (3- (N-morpholino)propanesulfonic acid), α-keto glutarate (αKG), succinate, pyruvate, malate, duroquinone, TMPD (N, N, N', N'-Tetramethyl-1, 4-phenylendiamin), ADP, malonate, rotenone, antimycin A, TTFA (Thenoyltrifluoroacetone), sodium azide, ascorbic acid, cytochrome c, decylubiquinone, haematoxylin, eosin, DPX, curcumin, temozolomide and DMSO were obtained from Sigma-Aldrich (USA). Xylene was purchased from SRL-India. Cycle Test Plus

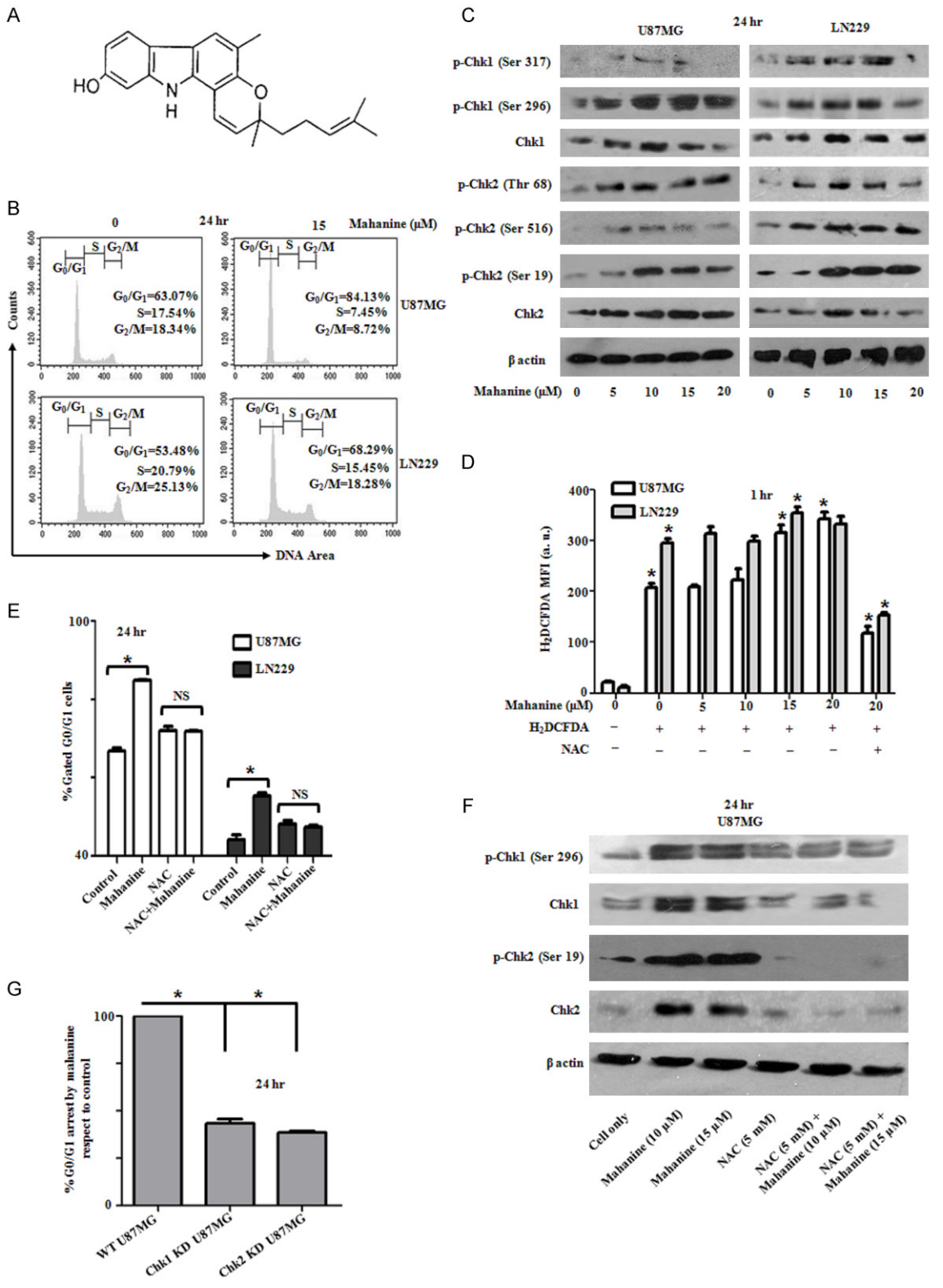

Figure 1. ROS-induced DNA damage response-mediated activation of checkpoint kinases in G0/G1 cell cycle arrest in glioblastoma multiforme. A. Chemical structure of mahanine isolated from *Murraya koenigii*. B. Mahanine (15 μM) induced G0/G1 phase cell cycle arrest in U87MG and LN229 cells. Enhancement of the % gated cells in the G0/G1 phase and subsequent reduction of cells in both S and G2/M phases indicated mahanine-induced G0/G1 phase cell cycle arrest. C. Mahanine induced upregulation of total Chk1 and Chk2 along with the phosphorylated

forms of those proteins. Enhancement of phosphorylations at Ser 317 and Ser 296 (for Chk1) and Thr 68, Ser 516 and Ser 19 (for Chk2) upon mahanine treatment indicated DDR. D. Generation of ROS upon treatment of mahanine for 1 hr in both LN229 and U87MG cells by H_2DCFDA staining. Elevated ROS was identified by enhanced mean fluorescence intensity value of H_2DCFDA. NAC (5.0 mM) was used as the scavenger of the produced ROS. E. NAC (5.0 mM)-mediated scavenging of ROS reduced the cell cycle arrest activity of mahanine upon 24 hr treatment in both the GBM cells. F. NAC (5.0 mM)-mediated scavenging of ROS could revert the DDR as no or reduced upregulation of total Chk1 and Chk2 and also their phosphorylated forms. G. Chk1 and Chk2 knocked down cells showed ~60-65% reduction in G0/G1 phase cell cycle arrest in mahanine-treated U87MG indicating the potential role of those checkpoint kinase proteins in mahanine-driven cell cycle dysfunction. Each value is the mean ± SD of three independent experiments. *P < 0.05, significant difference between two test groups.

kit for cell cycle analysis, cell recovery solution and matrigel were purchased from BD Bioscience (USA). SuperSignal West Pico imaging system was obtained from Thermo-scientific (USA).

Purification and characterization of mahanine

Mahanine was purified from fresh leaves of an Indian medicinal plant, *M. koenigii*, which belongs to the family of Rutaceae [26, 30]. HPLC, FAB-MS, ^{1}[H] and ^{13}[C] NMR spectral data analyses established its structure as mahanine (**Figure 1A**, Figure S1A, S1B) [22]. Cellular response mechanisms were identified with > 98% HPLC purified mahanine (Figure S1B).

Cell lines and astrocytes

Highly (U87MG) and moderately (LN229) invasive human glioblastoma cells were purchased from ATCC (USA) and grown in Iscove's Modified Dulbecco's Medium (IMDM) supplemented with 10% heat inactivated fetal calf serum (FCS) and 1% antibiotic-antimycotic solution in a humidified atmosphere at 37°C with 5% CO_2.

Primary cultures of astrocytes were established from cerebra of 1-2 day old rats [31]. Briefly, cells were seeded in 6-well plate (2×10^6 cells/well) and incubated in IMDM containing 10% FCS in a CO_2 incubator. The medium was changed on every 2 days and cytotoxicity was determined with 12th day post seeded cultures.

Cell cycle analysis

Cells (1×10^6) were treated with mahanine (0-20 μM) in presence or absence of esiRNA of Chk1/Chk2 and also in various oxygen environments for 24 hr. They were harvested and processed using Cell Cycle Test Plus kit. At least 20,000 cells were analyzed in FACS and analyzed by CellQuest Pro software (BD FACSCalibur).

Transfection

Cells (5×10^5) were pre-seeded for 24 hr in 6-well plate. Subsequently esiRNA transfection reagent containing esiRNA, nanopure water and NTER nanoparticle delivery solution was prepared. Control cells were in absence of esiRNA. This solution (200 μl) was added to each well and culture for 6 hr. Then the supernatant was aspirated and cells were subsequently cultured with fresh complete growth medium for another 12-15 hr before any drug treatment. Confirmation of esiRNA-mediated downregulation of target gene was evaluated by the Western blot analysis.

Measurement of intracellular ROS

Cells (1×10^6) were treated with mahanine (0-20 μM) for 1 hr and the levels of intracellular H_2O_2 were evaluated flow cytometrically by incubating with H_2DCFDA (10 μM) for 30 min at 37°C. This assay was also carried out in 1% and 8% oxygen environment in a hypoxia incubator (Thermo Scientific, USA). For the inhibition of ROS generation, cells were pretreated with N-acetyl cystine (NAC, 5.0 mM) for 1 hr before mahanine-treatment. 10,000 cells were analyzed [22]. Generation of ROS was also analyzed in presence of different mitochondrial ETC inhibitors (antimycin A, rotenone and TTFA).

Immunoblot analysis

Proteins were extracted from cells and quantified by Bradford method. An equivalent amount of protein (50 μg) was resolved by SDS-PAGE (7.5-12.5%) and electrotransferred to nitrocellulose membrane. The membrane was blocked by TBS-BSA, probed with primary antibody (1:1000 dilution) overnight at 4°C, washed with TBS-Tween-20 (0.1%) and incubated with the appropriate HRP-secondary antibody (1:1000-1:3000). Membrane was washed and immunereactive complex was identified by the West Pico chemiluminescence detector system [23].

Hypoxia induction assay

U87MG and LN229 cells were cultured in 1% O_2 environment for 24 hr [32] and incubated in absence and presence of mahanine with a definite concentration for 1 hr to estimate ROS and 24 hr for cell cycle analysis. Experiment was repeated in 8% oxygen environment as this was considered as brain tissue normoxic control [33].

Isolation of mitochondria

Mitochondria from U87MG was isolated by digitonin permeabilization method [34] with some modifications. Briefly, cells were washed with mitochondria-isolation buffer-I (pH 7.2) containing 210 mM mannitol, 70 mM sucrose, 5 mM HEPES, 0.02% BSA and 1 mM EGTA. Digitonin solution was added followed by equal volume of buffer-I. Cells were centrifuged at 3000 × g for 10 min and homogenize by Potter-Elvehjem homogenizer. Supernatant was isolated by the centrifugation at 1000 × g for 15 min and mitochondria was collected as pellet by centrifugation at 12000 × g for 15 min.

Measurement of oxygen consumption

U87MG and LN229 cells (2×10^6) and isolated mitochondria (0.3-0.5 mg/2 ml protein) were placed separately in the electrode chamber in respiratory medium (PBS, 2 ml) and oxygen consumption was measured in presence of glucose (10 mM) and mahanine (100 μM) by using Clark-type oxygen electrode fitted with Hansatech (GB) Oxygraph [35, 36].

Respiratory complex-inhibition by mahanine was confirmed by using specific respiratory complex substrates and inhibitors at 30°C. Substrates for complex-I [α-keto glutarate (10 mM), pyruvate (10 mM), malate (5.0 mM)]; complex-II [succinate (5.0 mM)]; complex-III [duroquinone (1.5 mM)]; complex-IV [TMPD (300 μM)], ATP synthase complex [ADP (0.4 mM)], different inhibitors e.g. 3 μM rotenone (complex-I), 10 mM malonate (complex-II) and 25 mM azide (complex-IV) were used at the indicated points.

Complex-III activity by spectrophotometric analysis

Activity of complex-III was measured spectrophotometrically following the reduction of cytochrome c by decylubiquinol at 550 nm [37, 38]. Decylubiquinol was prepared by reduction of 2, 3-dimethoxy-5-methyl-n-decyl-1, 4-benzoquinone (decylubiquinone) [39].

Active mitochondrial complexes were prepared from isolated mitochondria by dissolving in n-dodecyl-β-D-maltoside containing 10 mM potassium phosphate buffer using four freeze-thaw cycles. Mitochondrial protein (10-15 μg) was used as a source of complex-III. Complex-III-mediated reduction of cytochrome c (1 mM) was measured at 550 nm in presence of decylubiquinol (10 mM). Inhibition of complex-III specific activity was identified in presence/absence of mahanine (0-100 μM) in comparison to known complex-III inhibitor antimycin A (10 μg/ml) following the Beer-Lambert law equation [40]:

Complex-III activity = [{(ΔAbs_{550nm} without Antimycin – ΔAbs_{550nm} with Antimycin)/minute} × reaction volume]/[molar extinction co-efficient of cytochrome c × light path length × sample volume × protein concentration]

The fold change of cytochrome c reductase activity was graphically represented at 30 sec interval in presence and absence of antimycin A and mahanine by normalizing the every reading by the zero time point value.

Mitochondrial membrane potential assay

Cells (1×10^6) were treated in presence and absence of mahanine for 6 hr and the mitochondrial membrane-depolarization was determined with mitotracker deep red (100 nM) by incubating for 15 min at 37°C. Corresponding fluorescence was evaluated by FACS. ROS-dependent mitochondrial-depolarization was evaluated by the pretreatment of NAC (5.0 mM) for 1 hr before mahanine treatment. 10,000 cells were analyzed.

Measurement of cell death

GBM cells (1×10^6) were treated with mahanine for 24 hr and the dead cell population was determined by PI (5 μg/ml) staining for 15 min at 4°C through FACS. ROS-dependent plasma membrane disintegration was evaluated by the pretreatment of NAC (5.0 mM) for 1 hr before mahanine treatment. 10,000 cells were analyzed [22].

Cell proliferation analysis by MTT assay

GBM and astrocyte cells (1×10^4) were treated with mahanine (0-30 μM) for 48 hr and subse-

quently incubated with MTT (100 μg/ml) in fresh culture medium for 3 hr. Formazan crystals were dissolved in DMSO and OD was taken at 550 nm (Thermo Scientific, USA) [23].

Therapeutic strategy of mahanine in tumor xenograft study and in vivo identification of cell cycle progression

Female nude mice (NIH (s) nu/nu, 6-7 weeks old) were maintained in pathogen free conditions. U87MG cells (1×10^6, 200 μl) suspended in IMDM-matrigel (BD Bioscience, 1:1) were injected s.c. into the right hind limb. The tumor was allowed to develop for 20 days until it reached 200-250 mm^3, after that mahanine (100 mg/kg, 200 μl) in 10% DMSO containing NaCl (0.15 M) was administrated intraperitoneally per day for first 5 consecutive days and then five more treatment in alternative days in one group of tumor-carrying mice (n = 5). The control group of mice (n = 5) was treated with the same volume of vehicle only. Tumor volume was calculated by the formula: $L \times W^2/2$ (mm^3), where L = length and W = width using a Vernier caliper. On the 35^{th} day after the inoculation of the cancer cells, all the mice were sacrificed and the tumor xenografts were excised. The tumor cells were isolated from tumor tissue by collagenase type II-DNase I treatment [41]. Cells from the control and treated mice were subjected to cell cycle analysis by FACS. Tumor cells were also processed for the assessment of key G0/G1 phase cell cycle regulatory proteins by Western blot analysis.

Migration assay

Mahanine-treated and untreated U87MG and LN229 cells (1.5×10^6) were cultured to > 80% confluency in 6-well plate. Three separate scratch-wounds were made through the confluent cells and incubated further for 24 hr. Number of cells were calculated that moved into the scratched arena and image was taken by using phase contrast microscopy (Carl Zeiss, Germany) [23].

Connective tube formation assay

Thin layer of matrigel in IMDM (1:3) was formed in 24-well plate at 25°C. Control and mahanine-treated G0/G1 phase-arrested cells (5×10^4) were layered over matrigel in serum free medium. Images of connective tubes were recorded by phase contrast microscopy after 24 hr.

Differentiation assay

Mahanine-pretreated G0/G1 arrested and control cells (5×10^4) were diluted with matrigel (1:1) in IMDM and incubated for 5 days at 37°C in 24-well plate. Images were captured for radial outgrowth containing astrocytes/glial like cells by phase contrast microscopy [42].

To establish the astrocytic/glial differentiation in molecular level, cells were recovered from matrigel using recovery solution by incubating for 30 mins at 30°C with shaking. Cell suspension was centrifuged at 2000 rpm, fixed, permeabilized and incubated with anti-glial fibrillary acidic protein (GFAP). FITC-secondary antibody was added and analyzed by FACS [43]. At least 20,000 cells were analyzed.

Statistical analysis

All the data were from at least three independent experiments. Statistical analysis of data was performed using Graph Pad Prism 5 and Microsoft Excel software. The differences between the groups were analyzed by t-test or Mann-Whitney U-test. Comparisons between same cell line or mice group were done using paired t-test. Standard error bars represented the standard deviation of the mean (± SD). *$P < 0.05$, designated significant differences between the means of the control and the treated cells/mice, or two test groups.

Results

Mahanine induces G0/G1 phase cell cycle arrest and DDR in glioblastoma cells

Initially we wanted to determine whether mahanine has any role in cell cycle progression and regulation. Accordingly, we exposed two glioblastoma grade IV cells (U87MG and LN229) to various concentrations of mahanine for 24 hr and identified cell cycle arrest in the G0/G1 phase and the most effective concentration was 15 μM (**Figure 1B**, Figure S2). At this concentration, ~15% and ~20% excess cell was accumulated in G0/G1 phase in LN229 and U87MG respectively. A few cells were accumulated in the sub G0 phase indicating the initiation of apoptosis at 20 μM of mahanine (Figure S2).

Next we asked that what were the important pathways associated in cell cycle arrest. Accor-

dingly, we checked the DDR-related kinases Chk1/Chk2 and identified that both were upregulated in their total protein level and also activated through enhanced phosphorylations at Ser317 and Ser296 for Chk1 and Thr68, Ser516 and Ser19 for Chk2 upon treatment with mahanine (**Figure 1C**). The activation of Chk1/Chk2 was most prominent at 10-15 μM dose which corresponded to maximum cell cycle arrest. This result suggested that in some way DDR was related with the mahanine-induced G0/G1 phase cell cycle arrest.

Mahanine-induced intracellular ROS is major mediator for DDR and activation of Chk1/Chk2

Further we asked the cause of the DDR in presence of mahanine. Previously we had observed that mahanine is a potential pro-oxidant agent in leukemia, colorectal and pancreatic carcinoma [22, 24, 30]. This compound was also generated ROS efficiently within 1 hr both in U87MG and LN229 (**Figure 1D**). After demonstrating the involvement of DDR in the mahanine-treated G0/G1 arrest, we investigated the role of ROS in cell cycle arrest in GBM. NAC-mediated scavenging of ROS significantly reduced G0/G1 arrest, suggesting the participation of ROS in the mahanine-induced cell cycle arrest (**Figure 1E**).

We then hypothesized that ROS-mediated DDR is an important event for the mahanine-induced G0/G1 arrest. The scavenging of ROS by NAC efficiently suppressed mahanine-mediated upregulation of Chk1/Chk2 and phosphorylation at Ser296 for Chk1 and Ser19 for Chk2 (**Figure 1F**). This result indicated that mahanine-mediated accumulation of ROS was indeed an important factor for the generation of DDR in GBM. Furthermore, ~60-65% reduction of the cell cycle arrest in Chk1 and Chk2 knockdown U87MG demonstrated their critical importance in mahanine-mediated G0/G1 phase arrest (**Figure 1G**, Figure S3). Thus, we established that the ROS-mediated DDR triggered upregulation and activation of Chk1 and Chk2 which was essential for mahanine-mediated G0/G1 phase cell cycle arrest in GBM.

Mahanine triggers inhibition of complex-III in the mitochondrial electron transport chain

One of the most well accepted models of intracellular ROS production is the inhibition of ETC followed by leakage of electron into the mitochondrial lumen [36]. To further explore ETC as a target for mahanine, we investigated the mechanism of ROS production. Accordingly, we studied whether mahanine could inhibit the cellular and isolated mitochondrial oxygen consumption or not. Therefore, we measured the rate of oxygen consumption as indicated in slope under the curve after addition of mahanine in U87MG and LN229 (**Figure 2A**, **2B**). The reduction of the rate of oxygen consumption after addition of mahanine in both cells indicated a potential inhibition of ETC.

This result guided us to find out the answer of next obvious question that, which complex of mitochondrial ETC was inhibited by mahanine. Therefore, rate of oxygen consumption of isolated mitochondria from U87MG was measured in presence of complex-specific substrate followed by mahanine treatment (**Figure 2C-E**). Initial oxygen consumption in presence of α-keto glutarate (complex-I substrate) and ADP (ATP synthase substrate) was inhibited after addition of mahanine, indicated the probability of complex-I inhibition but addition of succinate (complex-II substrate) was unable to restart the respiration indicated that the ETC was indeed inhibited after complex-II (**Figure 2C**). This was further confirmed by addition of malonate (complex-II inhibitor). It was expected that if mahanine inhibited complex-I, then oxygen consumption rate starting with α-keto glutarate and succinate should not decrease much and addition of malonate should further reduce the respiratory rate but it was not the case (**Figure 2D**). To confirm the inhibition sites of mahanine after complex-II, measurement of oxygen consumption was started from the beginning with α-keto glutarate, succinate and ADP. It was identified that addition of mahanine inhibited the oxygen consumption rates which was sharply increased again by addition of TMPD (complex-IV substrate, **Figure 2E**), indicated that the mahanine induced inhibition in complex-III. Finally, mahanine-mediated complex-III inhibition was reconfirmed by the sequential addition of substrate and inhibitors of all the ETC complexes, where mahanine behaved like a potential inhibitor of duroquinone-induced sensitized mitochondrial complex-III in isolated mitochondria from both GBM cells (**Figure 2F**, Figure S4A). Once again the complex-III inhibitory property was firmly established as maha-

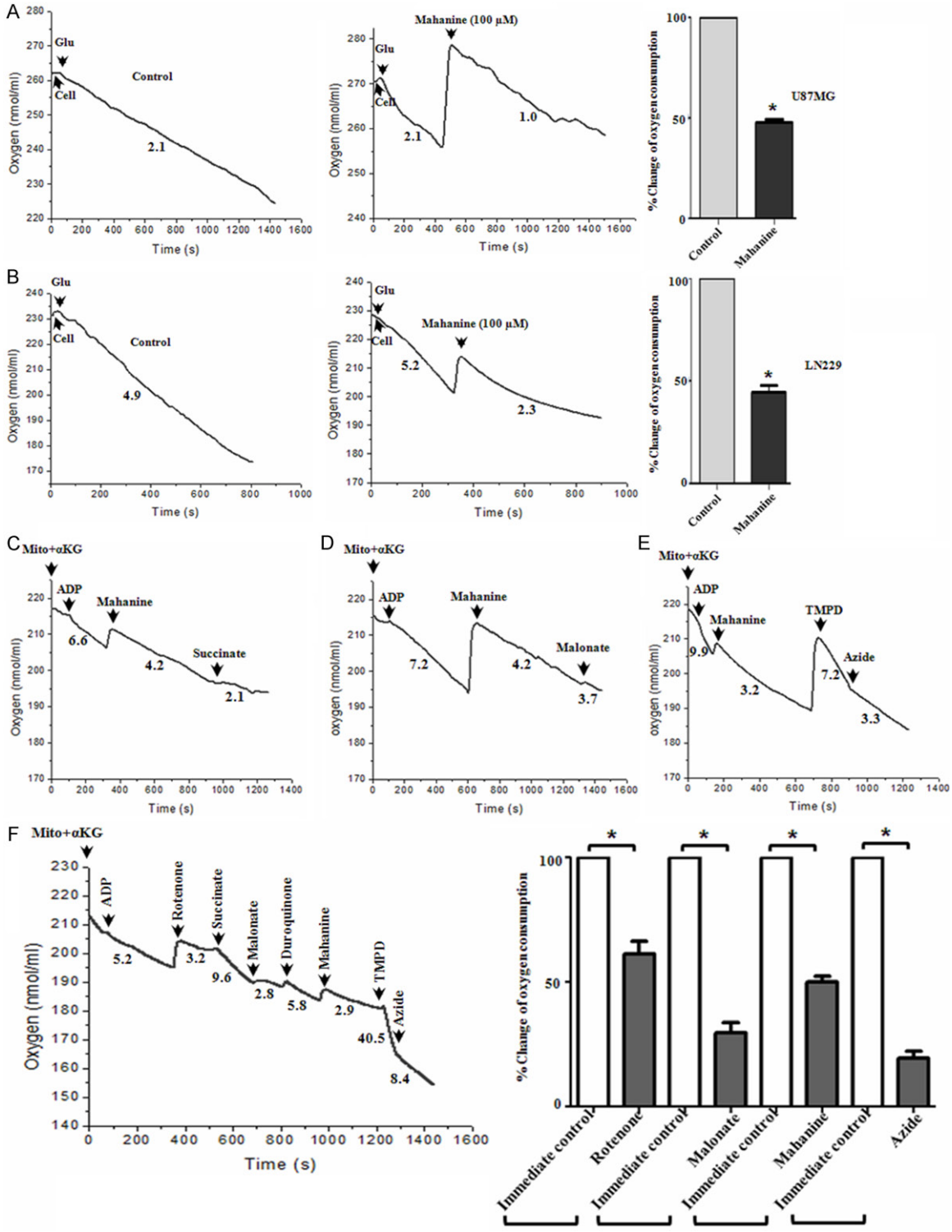

Figure 2. Inhibition of molecular oxygen consumption and respiration of cell was induced by blocking mitochondrial ETC at complex-III. A, B. Mahanine induced suppression of molecular oxygen consumption in both U87MG and LN229 cells identified by oxygraph analysis. Slope of the curve indicated the rate of oxygen consumption. Higher the value of the slope higher was the oxygen consumption. Reduction of slope after addition of mahanine indicated the inhibition of ETC. Bar graph represents the pictorial view for the inhibition of oxygen consumption in both the GBM cells. As mahanine was dissolved in absolute ethanol hence dissolved oxygen was higher. Due to this, after addition of mahanine total oxygen content became high in the reaction mixture, however inhibition by mahanine was evidenced by reduced slope. C. Succinate (complex-II substrate) could not initiate the mitochondrial oxygen

consumption in mahanine-inhibited ETC indicated the probable inhibition after complex-II. D. Malonate (complex-II inhibitor) could not further inhibit mitochondrial ETC which was previously inhibited by mahanine. This observation substantiated the fact that mahanine inhibited ETC after complex-II. E. Mahanine-induced inhibited mitochondrial ETC was activated upon the addition of TMPD (complex-IV substrate) and further inhibited by azide (complex-IV inhibitor), suggested the probable inhibition site between complex-II and complex-IV. F. Confirmation of complex-III inhibition by mahanine was established by sequential oxygraph analysis. Duroquinone (complex-III substrate)-mediated enhanced mitochondrial respiration was significantly blocked by mahanine hence proved this compound as a complex-III inhibitor. All the numerical values are included in the plot is representing the rate of oxygen consumption by the whole cell (per 2×10^6 cells) and/or live isolated mitochondria from U87MG cell (per mg). Bar graph represents the inhibition of oxygen consumption per addition of mitochondrial ETC inhibitors in different complexes with respect to the immediate control i.e. substrate-mediated activation per complexes. Each value is the mean ± SD of three independent experiments. $*P < 0.05$, significant difference between two test groups.

nine-mediated inhibition of ETC was not initiated further with succinate and duroquinone. However addition of TMPD started the ETC which was again inhibited by azide, complex-IV inhibitor (Figure S4B, S4C).

For the confirmation of complex-III inhibition by mahanine, spectrophotometric estimation of the conversion of cytochrome c from oxidized to reduced form was measured by determining the complex-III activity. Mahanine was identified again as a potential inhibitor of complex-III, depending on dose-dependent inhibition of specific activity of complex-III (**Figure 3A**). Antimycin A (10 μg/ml, 20 μM, complex-III inhibitor) exhibited almost equivalent inhibitory activity like 100 μM mahanine. Based on the specific activity, IC_{50} of mahanine for complex-III inhibition was ~24.68 μM within 5 minutes of kinetic reaction (**Figure 3B**).

Mahanine mediates ROS generation in hypoxia

Complex-III plays a major role in hypoxia-induced ROS generation [44, 45]. Antimycin A produces enhanced ROS in cells under hypoxic condition [44]. To reconfirm this phenomenon, we incubated the U87MG cells in 1% hypoxic environment for 24 hr and then they were treated separately with antimycin A, mahanine, rotenone and TTFA in combination or alone. Both antimycin A and mahanine could produce significant ROS whereas inhibitors of complex-I and II unable to produce ROS in hypoxic condition (Figure S5). We have observed concentration-dependent ROS accumulation in mahanine-treated GBM cells in this condition (**Figure 3C**).

Enhanced ROS induce higher G0/G1 phase cell cycle arrest and cell death in hypoxia

To further evaluate the importance of ROS in 1% hypoxic condition, cells were pretreated with NAC. There were significant hindrance of mahanine-induced G0/G1 arrest (**Figure 3D**), cell death (**Figure 3E**) and mitochondrial membrane depolarization (**Figure 3F**) in NAC-pretreated cells. These results indicated that mahanine-induced enhanced ROS was an essential factor for the cancer cell attenuation in hypoxic condition.

One of the major challenges in cancer chemotherapy is hypoxia-induced drug resistance [46]. To address this question, we used 1% and 8% oxygen environments as tumor hypoxia and tissue normoxia model respectively. Tissue absorption of oxygen is always limited and effective concentration is much below than aerial oxygen percentage. In brain, effective oxygen concentration is about 5-10% in tissue [33]. Mahanine exhibited higher pro-oxidant activity in hypoxic condition than tissue normoxia in GBM. Initial ROS level was higher in hypoxia than tissue normoxia. Due to the complex-III inhibition by mahanine, cells accumulated higher level of ROS (**Figure 3G**) which in turn responsible for enhanced cytotoxicity in hypoxic condition. This mahanine-induced enhanced ROS generation was also correlated with the moderately higher G0/G1 phase cell cycle arrest in hypoxia than 8% oxygen atmosphere (**Figure 3H**). Mahanine treatment accumulated about 6-7% higher amount cells in G0/G1 phase in hypoxia than tissue normoxia. These results indicated that hypoxia-induced drug resistance might not be a barrier for this novel complex-III inhibitor, mahanine.

Mahanine-induced G0/G1 arrest is confirmed by regulational change of cyclins/CDKs in GBM

For further confirmation of G0/G1 phase cell cycle arrest, we wanted to identify the regulation of different known G0/G1 transition related proteins. We observed that, CDC25A, early

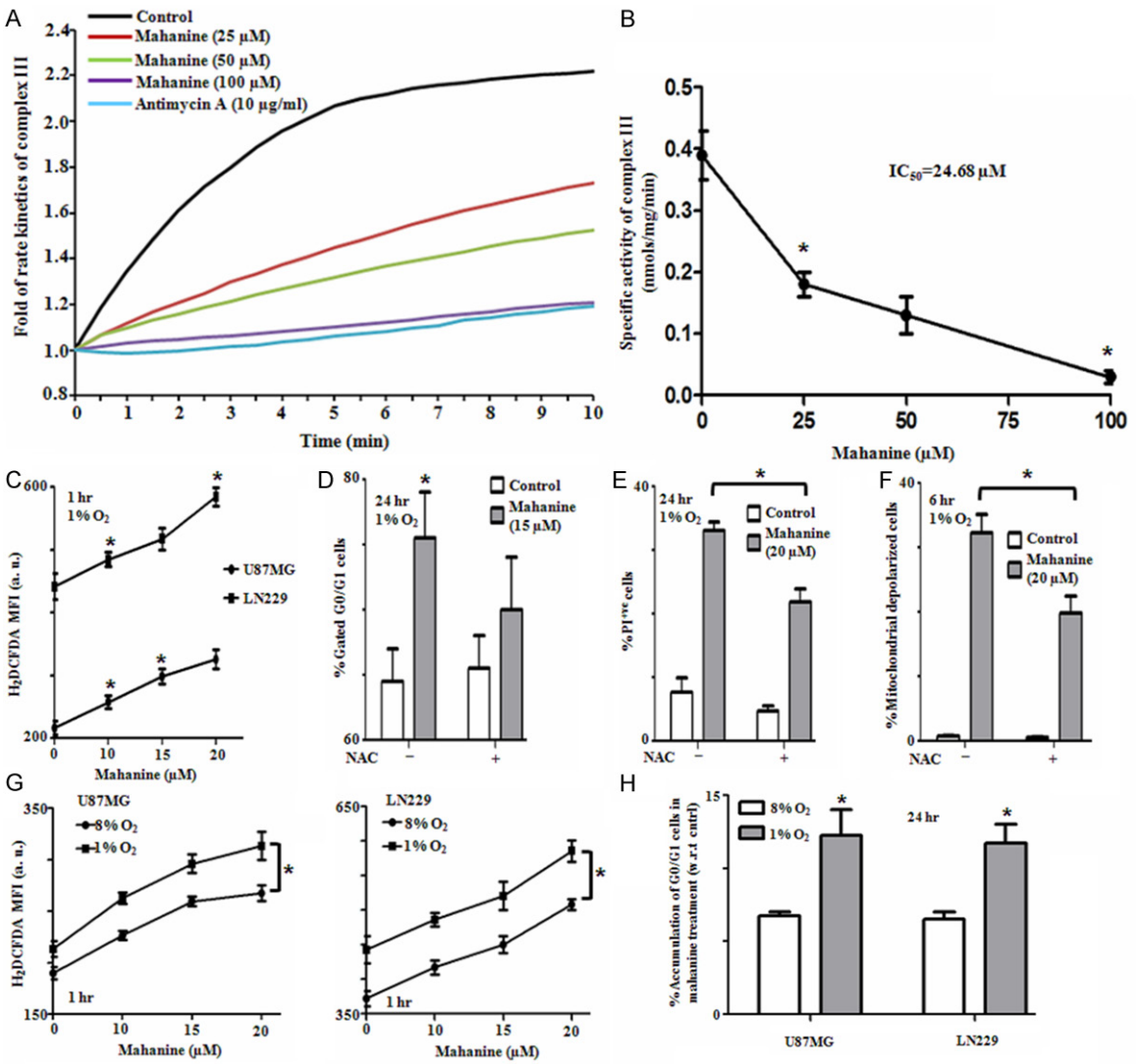

Figure 3. Confirmation of mahanine as mitochondrial complex-III inhibitor even in hypoxic condition. A. Dose dependent reduction of complex-III activity by mahanine according to the conversion of cytochrome c from oxidized to reduced form by spectrophotometric estimation at 550 nm. B. Identification of specific activity of complex-III in absence and presence (25, 50 and 100 μM) of mahanine and evaluation of IC_{50} as 24.68 μM for mahanine within 5 minutes. C. In 1% oxygen containing hypoxic conditions, mahanine induced ROS generation within 1 hr in both U87MG and LN229 cells identified by H_2DCFDA staining. D-F. Scavenging of mahanine-induced ROS by NAC in hypoxia (1% oxygen) rescued GBM cells from G0/G1 phase arrest (24 hr), cell death (24 hr) and mitochondrial membrane depolarization (6 hr) indicating the potential involvement of oxidative stress in mahanine-mediated cellular responses in hypoxia. G. Mahanine-treated U87MG and LN229 cells showed enhanced production of ROS in hypoxia (1% oxygen) than 8% oxygen-containing brain tissue normoxic condition. H. Mahanine-treated U87MG and LN229 cells showed moderately enhanced G0/G1 phase cell cycle arrest in hypoxia than brain tissue normoxic condition. Each value is the mean ± SD of three independent experiments. *$P < 0.05$, significant difference between two test groups.

G1 regulatory proteins e.g. cyclin D1, cyclin D3, CDK4 and CDK6 were downregulated upon treatment of mahanine (**Figure 4A**). Although, late G1 regulatory proteins, cyclin E and CDK2 were almost unaltered suggesting the importance of early G1 phase in this cell cycle arrest.

Superior anti-proliferative activity of mahanine than known chemotherapeutic agents, even in temozolomide resistant GBM cells with low toxicity

After initial cell cycle arrest in glioblastoma cells by mahanine, concentration-dependent

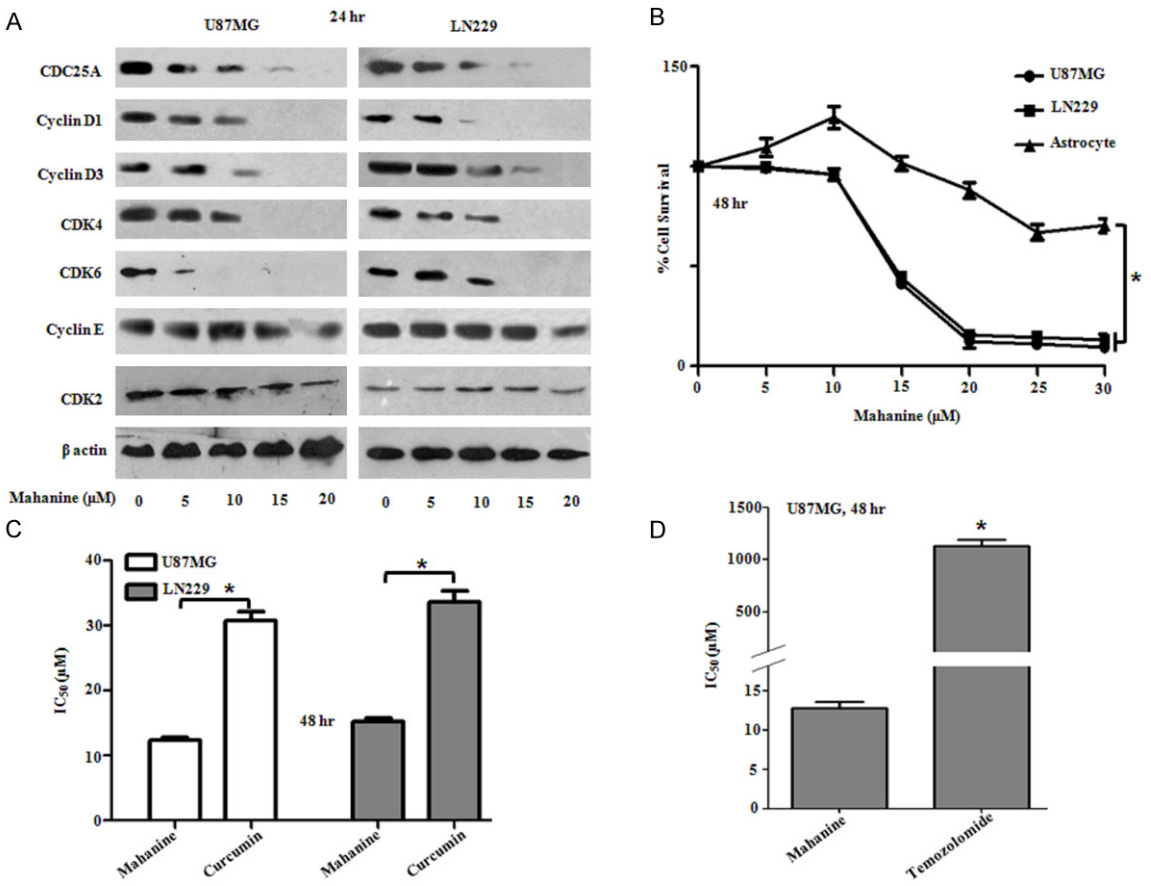

Figure 4. G0/G1-transition regulatory proteins were positively regulated in the course of cell cycle arrest and apoptosis. A. Mahanine induced downregulation of CDC25A, cyclin D1, cyclin D3, CDK4 and CDK6 in both LN229 and U87MG cells confirmed the G0/G1 cell cycle arrest in molecular level. B. Concentration-dependent inhibition of cell survival of mahanine-treated U87MG and LN229 glioblastoma cells after 48 hrs wherein normal astrocytes were used as control. Mahanine-induced less inhibition of cell survival indicated relative nontoxicity of mahanine towards normal astrocytes. C. Mahanine showed enhanced cytotoxicity than curcumin identified by IC_{50} value in both the GBM cells upon 48 hr treatment. D. Susceptibility of temozolomide resistant U87MG cell towards mahanine, identified by ~80 fold reduced IC_{50} value upon 48 hr treatment. Each value is the mean ± SD of three independent experiments. *P < 0.05, significant difference between two test groups.

cell death was observed in both GBM cells. They showed more sensitivity towards mahanine than normal lineage astrocytes (**Figure 4B**). Thus the selectivity of mahanine towards cancer cells with minimal adverse toxicity towards normal astrocytes was demonstrated.

Next we wanted to compare the anti-proliferative activity of mahanine with two selected drugs namely curcumin and temozolomide. Mahanine showed enhanced anti-proliferative activity in both GBM cells as reflected by lower IC_{50} value (~12-15 μM) than curcumin (~30-35 μM) after 48 h treatment (**Figure 4C**).

Even temozolomide-resistant U87MG cells [19, 47] showed much higher susceptibility towards mahanine as indicated by ~80 fold less IC_{50} value after 48 hr (**Figure 4D**) indicating that mahanine may consider to be a better chemotherapeutic agents for GBM with low adverse toxicity.

Mahanine restricts the cell cycle progression of cancer cells in G0/G1 phase transition in vivo model

To confirm the *in vivo* therapeutic efficacy of mahanine, we have generated xenograft tumor model in athymic nude mice by transplanting U87MG cells. After the treatment of mice with mahanine, progression of tumor was significantly restricted (**Figure 5A**, **5B**). Furthermore, mahanine-treated mice showed reduction in

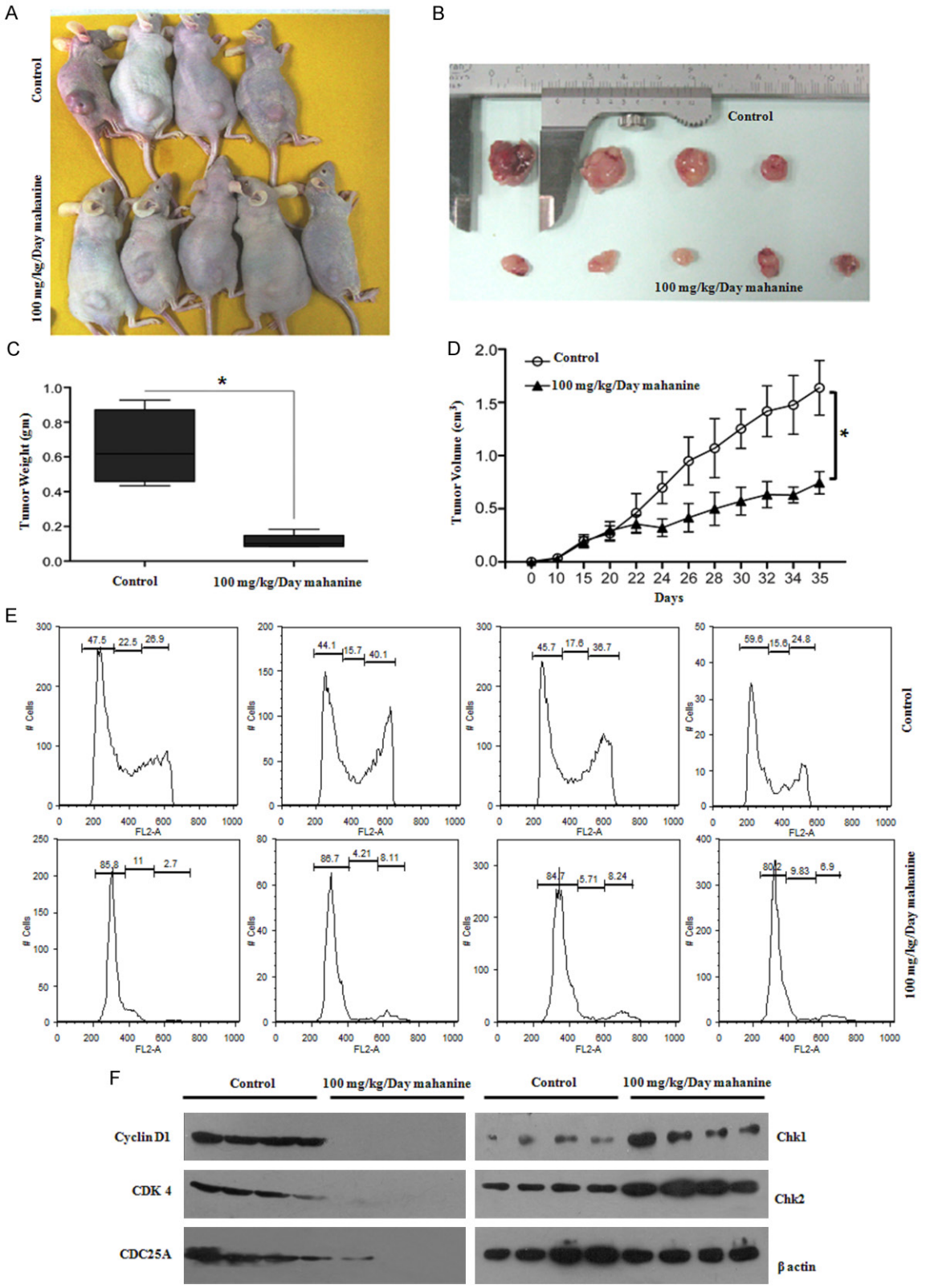

Figure 5. *In vivo* therapeutic efficacy of mahanine to reduce xenograft tumor and confirmation of G0/G1 arrest in nude mice model. A. Pictorial representation of mahanine-mediated regression of U87MG xenograft tumor in nude mice. B. Pictorial representation of reduced size of excised tumor in mahanine-treated mice than control set. C. Treatment of mahanine induced the reduction of tumor weight in treated mice than control group. D. The graphi-

cal representation indicated the reduced-progressiveness of tumor in mahanine-treated mice for the 35 (from the date of tumor cell inoculation) days of incubation period. E. DNA profiling of isolated tumor cells from control and mahanine-treated group of mice indicated that mahanine restricted the cell cycle progression of tumor cells in G0/G1 phase transition. Each histogram plot of cell cycle distribution indicated each tumor. F. Confirmation of *in vivo* G0/G1 phase cell cycle arrest by downregulation of cyclin D1, CDK4, CDC25A and upregulation of Chk1, Chk2 in mahanine-treated tumor cells. Each lane in Western blot analysis indicated each tumor cell extract. Each value is the mean ± SD of three independent experiments. *$P < 0.05$, significant difference between two test groups.

the weight of tumor mass (**Figure 5C**) and also reduced gradual progression of tumor throughout the incubation period of 35 days (**Figure 5D**).

To establish the *in vitro* mechanisms elicited by mahanine for G0/G1 arrest in *in vivo* condition, cell cycle analysis was performed of tumor-isolated cells and identified that mahanine restricted those cells in G0/G1 phase. FACS analysis indicated that about 85% cells were accumulated in G0/G1 phase after the therapeutic course of mahanine, whereas only about 50% cells were there in vehicle-treated tumor (**Figure 5E**). This *in vivo* G0/G1 arrest was confirmed by the down regulation of cyclin D1, CDK4, CDC25A and upregulation of Chk1, Chk2 in mahanine-treated tumor (**Figure 5F**).

Mahanine-induced G0/G1 arrested cells show significant inhibition of different oncogenic properties in vitro and in vivo

Cancer cells have a variety of oncogenic characteristics facilitating their rapid growth/proliferation. We investigated whether mahanine-induced G0/G1 arrested cells displayed an inhibition of any such oncogenic properties. Mahanine-induced G0/G1 arrested GBM cells illustrated a significantly reduced capacity to migrate (**Figure 6A**). The arrested U87MG also exhibited a reduced capacity for connective tube formation between cells (**Figure 6B**) indicating less invasiveness. Interestingly, mahanine-induced G0/G1 arrested cells differentiated from epithelial-like cells and formed astrocytes/glial-like radial outgrowth-containing structures in matrigel (**Figure 6C**). The upregulated level of GFAP in G0/G1 arrested U87MG confirmed the differentiation process by mahanine (**Figure 6D**).

Next we wanted to address whether the effect of mahanine-induced G0/G1 phase arrest was reversible or not. To confirm that we implanted G0/G1 arrested cells into the nude mice along with the control cells and observed for 30 days to measure tumor formation. Mahanine-treated G0/G1 arrested U87MG showed reduced capacity to form *in vivo* xenograft tumor identified by tumor size, volume and weight (**Figure 6E**, Figure S6A, S6B). Reduced formation of this tumor was further confirmed by the H&E staining, as it was identified that compactness of the cells and number of nucleus were reduced in the G0/G1 arrested U87MG-mediated tumor than control (**Figure 6F**). For each experiment, cell cycle profile of control and G0/G1-arrested cells were checked and only arrested cells were injected for tumor transplantation where subG0 population was < 5% (Figure S6C). All these observations suggested that mahanine-induced cell cycle arrest could potentially revert the various oncogenic properties of malignant cells and hence might consider as a potential chemotherapeutic agent.

Discussion

Various gene polymorphisms and mutations have an impact on DNA repair and cell cycle regulation in glioblastoma [48]. Therefore, an effect on cell cycle progression might be a useful therapeutic strategy against this cancer. The main achievement of the present study is to introduce a carbazole alkaloid which induced cell cycle arrest in GBM in the G0/G1 phase transition through ROS production. The ROS was mainly generated through the inhibition of complex-III in mitochondrial ETC. Thus establishing complex-III of ETC is one of the potential targets of mahanine. This accumulated ROS further activated the DDR which then upregulated and activated Chk1 and Chk2 leading to cell cycle arrest in GBM cells conclusively confirmed both *in vitro* and *in vivo* experiments.

Mitochondrial ETC is the most crucial system for energy generation and the major process for the oxidative phosphorylation [49-51]. Four different protein complexes in the ETC are located in the inner mitochondrial membrane.

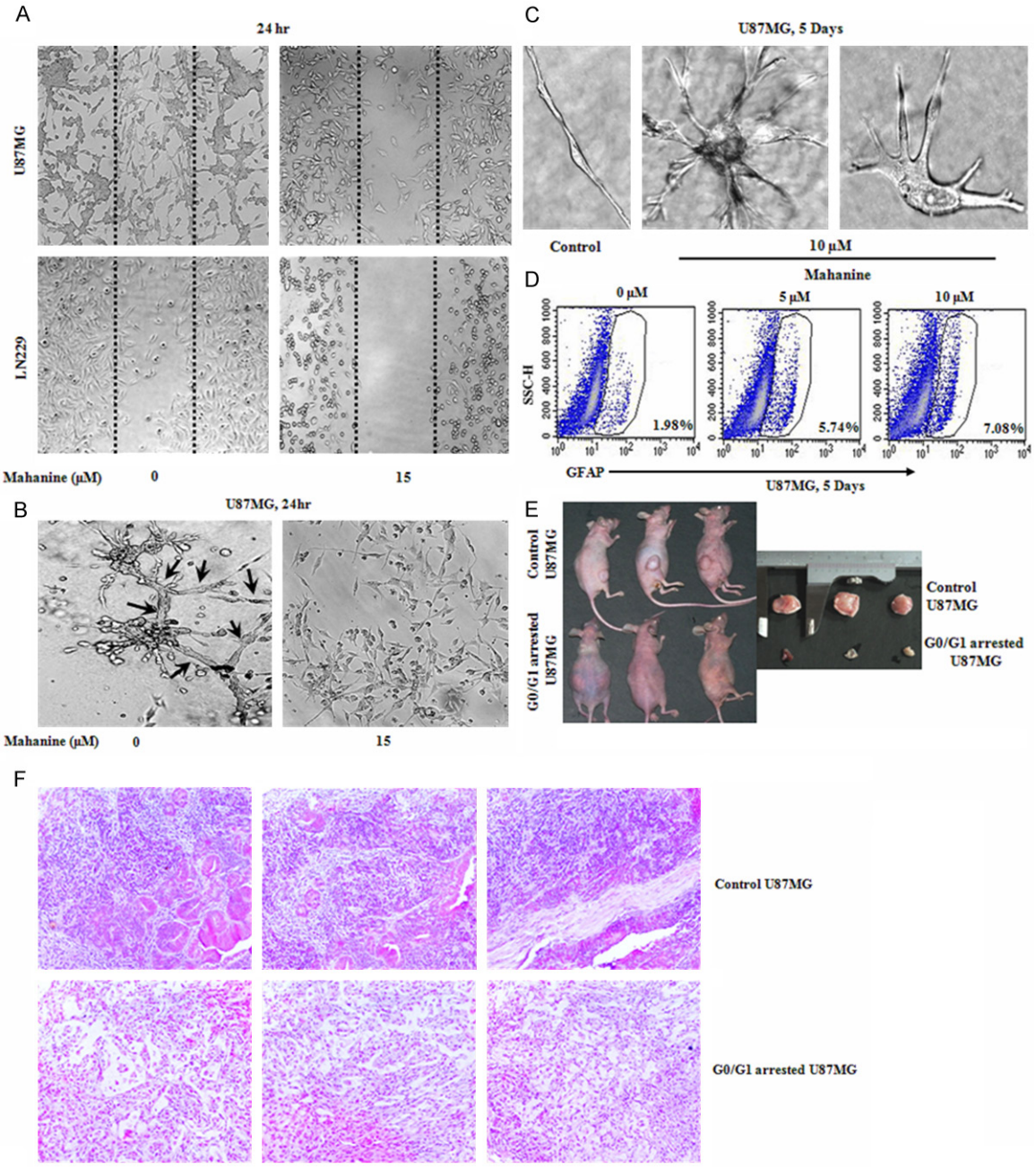

Figure 6. G0/G1 phase arrested cells showed altered functional activity *in vitro* and *in vivo*. A. Inhibition of *in vitro* migration of both mahanine (15 μM)-induced G0/G1 arrested U87MG and LN229 cells in scratched arena (in between dotted lines). B. Mahanine (15 μM)-induced G0/G1 phase arrested U87MG cells had lower potential to form connection tubes in *in vitro* matrigel assay. The connection tubes were indicated by '→'. Reduction of this tubular connection indicated the minimization of invasiveness of cancer. C. Mahanine (10 μM)-induced conversion of undifferentiated epithelial like population of U87MG cell to well differentiated astrocytes or glial like structure with radial outgrowth by microscopic after the incubation in matrigel for 5 days. D. Overexpression of GFAP, the astrocytes or glial differentiation marker protein, in the mahanine-induced G0/G1 arrested U87MG cells after 5 days culture in matrigel. E. U87MG cell (control) produced extensive growth of xenograft tumor in right flank of nude mice compared to mahanine-treated G0/G1 arrested U87MG cell. F. H&E staining indicated that compact cellular arrangement and high density of nucleus in control U87MG-induced tumor section compared to G0/G1 phase arrested U87MG-mediated tumor in athymic nude mice.

Electrons pass through the complex-I to complex-IV with the help of electron carriers e.g. ubiquinone and cytochrome c. This process is essential for the generation of electrochemical

proton gradient through the inner membrane. Complex-V, the F_1F_0-ATPase, generate ATP from ADP and inorganic phosphate by utilizing the energy from the proton gradient, which provides fundamental energy molecule. If ETC is blocked in any complex in the chain then electrons are leaked out and come into the lumen and readily reduce molecular O_2 into superoxide anion, H_2O_2 and other species. These ROS are essential for initial mitochondrial and then cellular damages [49].

Mahanine is an established pro-oxidant agent in cancers [22, 24, 30] including GBM. Here we showed that the ROS is generated due to the leakage of electrons as mahanine inhibits complex-III in ETC in GBM which is responsible for activation of the DDR. Such activation triggered upregulation and activation of Chk1 and Chk2 as characterized by the activation phosphorylation at Ser317/296 (Chk1) and Thr68, Ser516/19 (Chk2). Scavenging of ROS by NAC pre-treatment significantly decreased the potency of the compound to induce DDR and cell cycle arrest. Chk1 and Chk2 are structurally dissimilar however functionally related to serine/threonine kinases which are activated in response to different genotoxic insults [52-54]. The major role of Chk1 and Chk2 is to transmit the checkpoint signals from the initial checkpoint-kinases ATM and ATR [55, 56]. Chk2 is expressed throughout the cell cycle process [57] and activated majorly by ATM in response to double-strand DNA breaks. However, Chk1 protein is significantly restricted to S and G2 phases [58] and activated in response to DNA damage or delayed replication.

Mahanine-induced G0/G1 phase cell cycle arrest was further confirmed by downregulation of CDC25A and early G1-regulatory cyclin D1/cyclin D3 and their associated kinases CDK4/CDK6, but the late G1-regulatory kinase CDK2 and the cyclin E level were unaltered. Down regulation of CDC25A might also related with the Chk1/Chk2 activation as hyperphosphorylation induced proteasomal degradation of CDC25A induced by checkpoint kinases. Mahanine induced expression of the epigenetically silenced tumor-suppressor gene RASSF1A and blocked cyclin D1 expression in prostate cancer [28].

Tamoxifen, a complex-I inhibitor is used in premenopausal hormone-positive breast cancer. Metformin (complex-I inhibitor), porphyrin photosensitizers and N-(4-Hydroxyphenyl) retinamide (complex-IV inhibitors) are in phase III clinical trial in cancers [49]. Complex-III inhibitor, resveratrol has completed phase II trial [49]. Although other mitochondrial complex inhibitors are reported, but due to severe toxicity problem, they are not considered as ideal chemotherapeutic agents in cancers. Mahanine has no adverse toxic effects [22, 23] and it shows activity against several malignancies, so we may use this mitochondrial complex-III inhibitor as a novel chemotherapeutic agent. Potentiality of mahanine was increased because it showed equivalent efficacy in same cellular pathway both *in vitro* and *in vivo*.

Hypoxia is a signature mark for the different solid tumors including GBM. Oxygen tension is around 0.1-10% in GBM malignant tissue [33]. In contrast, oxygen level is in higher range from 5-10% in normal brain [33]. Oxygen sensing in hypoxia is a major factor for redox balance and adaptation [59]. Hypoxia-induced ROS production is highly controlled by well-regulated machinery in the mitochondrial ETC. This ROS plays an important role for the stabilization of HIF1α and thereby control the signal-transduction pathway in this stressed condition [59]. Complex-III plays a most important role in hypoxia-induced ROS generation [44, 45]. Relative stabilization of ubisemiquinone in complex-III Q-cycle in hypoxic-stress produces higher ROS by the conversion of molecular oxygen to superoxide radical and H_2O_2, the major molecular-mediator of redox alteration [44]. Hence mainly the complex-III inhibitor like antimycin A can produce excessive ROS in hypoxia [44, 60]. However, in contrast to antimycin A, myxothiazol (another complex-III inhibitor) along with complex-I (rotenone) and complex-II (TTFA) inhibitors cannot produce ROS in hypoxia as these cannot stabilise the ubisemiquinone form in Q-cycle [44, 60]. As the novel complex-III inhibitor, mahanine generated significant ROS in hypoxia then this might be hypothesized that it also can stabilize ubisemiquinone form. This ROS had also been identified as important molecular-mediator for mahanine-induced cell cycle arrest, cell death and mitochondrial membrane depolarization even in hypoxia. As mahanine accumulated enhanced ROS in hypoxia, this oxidative burst played an important role for higher G0/G1 phase arrest and inhibition of cancer cell proliferation than tissue normoxic

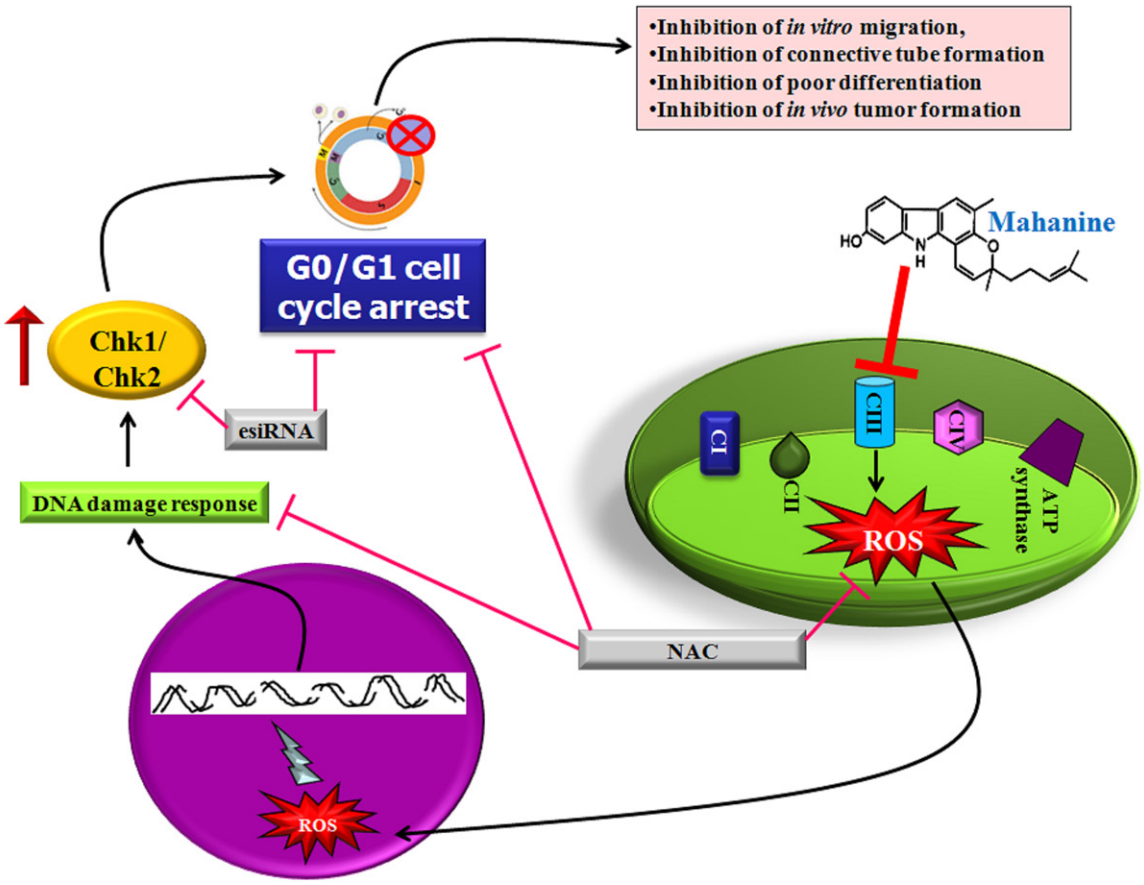

Figure 7. Schematic representation of oxidative imbalance-induced G0/G1 phase cell cycle arrest in GBM by mahanine-mediated mitochondrial complex-III inhibition.

condition. Hypoxia-induced drug resistance are common phenomenon and we strongly believe that inhibition in specific site of complex-III would be a better strategy to manage cancer in hypoxic-milieu in tumor microenvironment. As mahanine did not show any adverse toxicity *in vitro* and *in vivo* like reported ETC blocker, it could be a useful agent in drug irresponsive hypoxic condition.

Mahanine also displayed a potent capacity to restrict growth at G0/G1 and induce cell death even in the most oncogenic EGFRvIII mutation [16, 17] in GBM (data not shown). Therefore, this non-toxic carbazole alkaloid may be considered as a potential alternative treatment of this intractable disease. Mahanine, an inhibitor of *in vitro* cell migration and cell-cell connective tube formation and *in vivo* tumor generation ability, supported its potential anti-glioma role. Additionally, the differentiation of mahanine-treated cells arrested in the G0/G1 phase, identified as astrocyte or glial-like structure, generated from epithelial morphology, makes this molecule an interesting agent. Therefore, it is hypothesized that mahanine is capable of forcing G0/G1 phase-arrested cells through the G0 phase, as evidenced by their differentiation.

Based on all these observations, we strongly suggest that mahanine is a novel mitochondrial complex-III inhibitor of ETC with potent anti-GBM activity both in *in vitro* and *in vivo* model triggering cell death by inducing cell cycle arrest through ROS mediated activation of DNA damage check point (**Figure 7**). As it showed high therapeutic potential in several other cancer models, accordingly this is a potential agent for future chemotherapy. For the first time, complex-III of ETC has been identified as the potential target of this nontoxic molecule. Therefore, we propose the introduction of this molecule alone or in combination with conventional chemotherapeutic agents in the treatment of grade IV brain tumor, even in the hypoxic-microenvi-

ronment, temozolomide-resistant and EGFRvIII-mutation-bearing conditions. However more studies are needed for further validation.

Acknowledgements

We sincerely acknowledge CSIR-IICB, CSIR (IAP-0001, HCP004, NMITLI, TLP-004), ICMR (GAP 294) and DBT (GAP 235), Govt. of India. CM is grateful to financial support by Sir J.C. Bose National Fellowship, DST and mutual grant from ICMR and German Cancer Research Centre and mutual grant from CSIR and Charité - Universitätsmedizin Berlin. We are also very much grateful to Prof. Manju Ray and Dr. Alok Ghosh, Bose Institute, Kolkata for supporting us to use oxygraph instrument for measurement of mitochondrial respiration. We are thankful to Dr. Sumantra Das, CSIR-IICB for helping us astrocytes isolation and culture.

Disclosure of conflict of interest

None.

Address correspondence to: Chitra Mandal, Cancer Biology and Inflammatory Disorder Division, Council of Scientific and Industrial Research (CSIR)-Indian Institute of Chemical Biology, 4, Raja S.C. Mullick Road, Jadavpur, Kolkata-700032, India. E-mail: chitra_mandal@yahoo.com

References

[1] Halliwell B. Reactive species and antioxidants. Redox biology is a fundamental theme of aerobic life. Plant Physiol 2006; 141: 312-22.

[2] Simon HU, Haj-Yehia A, Levi-Schaffer F. Role of reactive oxygen species (ROS) in apoptosis induction. Apoptosis 2000; 5: 415-8.

[3] Giordano S, Lee J, Darley-Usmar VM, Zhang J. Distinct effects of rotenone, 1-methyl-4-phenylpyridinium and 6-hydroxydopamine on cellular bioenergetics and cell death. PLoS One 2012; 7: e44610.

[4] Wang CH, Wang CC, Huang HC, Wei YH. Mitochondrial dysfunction leads to impairment of insulin sensitivity and adiponectin secretion in adipocytes. FEBS J 2013; 280: 1039-50.

[5] Collins K, Jacks T, Pavletich NP. The cell cycle and cancer. Proc Natl Acad Sci U S A 1997; 94: 2776-8.

[6] Malumbres M, Barbacid M. Cell cycle, CDKs and cancer: a changing paradigm. Nat Rev Cancer 2009; 9: 153-66.

[7] Schafer K. The cell cycle: a review. Vet Pathol 1998; 35: 461-78.

[8] Niida H, Murata K, Shimada M, Ogawa K, Ohta K, Suzuki K, Fujigaki H, Khaw AK, Banerjee B, Hande MP, Miyamoto T, Miyoshi I, Shirai T, Motoyama N, Delhase M, Appella E, Nakanishi M. Cooperative functions of Chk1 and Chk2 reduce tumour susceptibility in vivo. EMBO J 2010; 29: 3558-70.

[9] Schmitt E, Paquet C, Beauchemin M, Bertrand R. DNA-damage response network at the crossroads of cell-cycle checkpoints, cellular senescence and apoptosis. J Zhejiang Univ Sci B 2007; 8: 377-97.

[10] Demir MK, Hakan T, Akinci O, Berkman Z. Primary cerebellar glioblastoma multiforme. Diagn Interv Radiol 2005; 11: 83-6.

[11] Ohgaki H, Dessen P, Jourde B, Horstmann S, Nishikawa T, Di Patre PL, Burkhard C, Schüler D, Probst-Hensch NM, Maiorka PC, Baeza N, Pisani P, Yonekawa Y, Yasargil MG, Lütolf UM, Kleihues P. Genetic pathways to glioblastoma: a population-based study. Cancer Res 2004; 64: 6892-9.

[12] Stewart LA. Chemotherapy in adult high-grade glioma: a systematic review and meta-analysis of individual patient data from 12 randomised trials. Lancet 2002; 359: 1011-8.

[13] Wolburg H, Noell S, Fallier-Becker P, Mack AF, Wolburg-Buchholz K. The disturbed blood-brain barrier in human glioblastoma. Mol Aspects Med 2012; 33: 579-89.

[14] Pietsch T, Wiestler OD. Molecular neuropathology of astrocytic brain tumors. J Neurooncol 1997; 35: 211-22.

[15] Collins VP. Cellular mechanisms targeted during astrocytoma progression. Cancer Lett 2002; 188: 1-7.

[16] Heimberger AB, Hlatky R, Suki D, Yang D, Weinberg J, Gilbert M. Prognostic effect of epidermal growth factor receptor and EGFRvIII in glioblastoma multiforme patients. Clin Cancer Res 2005; 11: 1462-6.

[17] Heimberger AB, Suki D, Yang D, Shi W, Aldape K. The natural history of EGFR and EGFRvIII in glioblastoma patients. J Transl Med 2005; 3: 38.

[18] Wen PY, Kesari S. Malignant gliomas in adults. N Engl J Med 2008; 359: 492-507.

[19] Henson JW. Treatment of glioblastoma multiforme: a new standard. Arch Neurol 2006; 63: 337-41.

[20] Dhandapani KM, Mahesh VB, Brann DW. Curcumin suppresses growth and chemoresistance of human glioblastoma cells via AP-1 and NFkappaB transcription factors. J Neurochem 2007; 102: 522-38.

[21] Mondal S, Bandyopadhyay S, Ghosh MK, Mukhopadhyay S, Roy S, Mandal C. Natural products: promising resources for cancer drug discovery. Anticancer Agents Med Chem 2012; 12: 49-75.

[22] Bhattacharya K, Samanta SK, Tripathi R, Mallick A, Chandra S, Pal BC, Shaha C, Mandal C. Apoptotic effects of mahanine on human leukemic cells are mediated through crosstalk between Apo-1/Fas signaling and the Bid protein and via mitochondrial pathways. Biochem Pharmacol 2010; 79: 361-72.
[23] Mandal C, Pal BC, Bhattacharya K, Samanta SK, Sarkar S, Das R. Process for the isolation of organic compounds useful for the treatment of cancer. US patent 2014; Pub No: US863-7679 B2.
[24] Sarkar S, Dutta D, Samanta SK, Bhattacharya K, Pal BC, Li J, Datta K, Mandal C, Mandal C. Oxidative inhibition of Hsp90 disrupts the super-chaperone complex and attenuates pancreatic adenocarcinoma in vitro and in vivo. Int J Cancer 2013; 132: 695-706.
[25] Roy MK, Thalang VN, Trakoontivakorn G, Nakahara K. Mahanine, a carbazole alkaloid from Micromelum minutum, inhibits cell growth and induces apoptosis in U937 cells through a mitochondrial dependent pathway. Br J Pharmacol 2005; 145: 145-55.
[26] Das R, Bhattacharya K, Samanta SK, Pal BC, Mandal C. Improved chemosensitivity in cervical cancer to cisplatin: Synergistic activity of mahanine through STAT3 inhibition. Cancer Lett 2014; doi: 10.1016/j.canlet. 2014. 05. 005.
[27] Sinha S, Pal BC, Jagadeesh S, Banerjee PP, Bandyopadhaya A, Bhattacharya S. Mahanine inhibits growth and induces apoptosis in prostate cancer cells through the deactivation of Akt and activation of caspases. Prostate 2006; 66: 1257-65.
[28] Jagadeesh S, Sinha S, Pal BC, Bhattacharya S, Banerjee PP. Mahanine reverses an epigenetically silenced tumor suppressor gene RASSF1A in human prostate cancer cells. Biochem Biophys Res Commun 2007; 362: 212-7.
[29] Samanta SK, Dutta D, Roy S, Bhattacharya K, Sarkar S, Dasgupta AK, Pal BC, Mandal C, Mandal C. Mahanine, A DNA Minor Groove Binding Agent Exerts Cellular Cytotoxicity with Involvement of C-7-OH and -NH Functional Groups. J Med Chem 2013; 56: 5709-21.
[30] Das R, Bhattacharya K, Sarkar S, Samanta SK, Pal BC, Mandal C. Mahanine synergistically enhances cytotoxicity of 5-fluorouracil through ROS-mediated activation of PTEN and p53/p73 in colon carcinoma. Apoptosis 2013; 19: 149-64.
[31] Dasgupta A, Das S, Sarkar PK. Thyroid hormone promotes glutathione synthesis in astrocytes by up regulation of glutamate cysteine ligase through differential stimulation of its catalytic and modulator subunit mRNAs. Free Radic Biol Med 2007; 42: 617-26.
[32] Batra S, Reynolds CP, Maurer BJ. Fenretinide cytotoxicity for Ewing's sarcoma and primitive neuroectodermal tumor cell lines is decreased by hypoxia and synergistically enhanced by ceramide modulators. Cancer Res 2004; 64: 5415-24.
[33] McCord AM, Jamal M, Shankavaram UT, Lang FF, Camphausen K, Tofilon PJ. Physiologic oxygen concentration enhances the stem-like properties of CD133+ human glioblastoma cells in vitro. Mol Cancer Res 2009; 7: 489-97.
[34] Moreadith RW, Fiskum G. Isolation of mitochondria from ascites tumor cells permeabilized with digitonin. Anal Biochem 1984; 137: 360-7.
[35] Zhang J, Nuebel E, Wisidagama DR, Setoguchi K, Hong JS, Van Horn CM, Imam SS, Vergnes L, Malone CS, Koehler CM, Teitell MA. Measuring energy metabolism in cultured cells, including human pluripotent stem cells and differentiated cells. Nat Protoc 2012; 7: 1068-85.
[36] Ghosh A, Bera S, Ghosal S, Ray S, Basu A, Ray M. Differential inhibition/inactivation of mitochondrial complex-I implicates its alteration in malignant cells. Biochemistry 2011; 76: 1051-60.
[37] Luo C, Long J, Liu J. An improved spectrophotometric method for a more specific and accurate assay of mitochondrial complex-III activity. Clin Chim Acta 2008; 395: 38-41.
[38] Luo H, Yang A, Schulte BA, Wargovich MJ, Wang GY. Resveratrol Induces Premature Senescence in Lung Cancer Cells via ROS-Mediated DNA Damage. PLoS One 2013; 8: e60065.
[39] Fisher N, Bourges I, Hill P, Brasseur G, Meunier B. Disruption of the interaction between the Rieske iron-sulfur protein and cytochrome b in the yeast bc1 complex owing to a human disease-associated mutation within cytochrome b. Eur J Biochem 2004; 271: 1292-8.
[40] Magri S, Fracasso V, Rimoldi M, Taroni F. Preparation of yeast mitochondria and in vitro assay of respiratory chain complex activities. Protocol Exchange 2010; doi: 10.1038/nprot. 2010. 25.
[41] Modzelewski AR, Davies P, Watkins CS, Auerbach R, Chang M, Johnson SC. Isolation and identification of fresh tumor-derived endothelial cells from a murine RIF-1 fibrosarcoma. Cancer Res 1994; 54: 336-9.
[42] Grefte S, Vullinghs S, Kuijpers-Jagtman AM, Torensma R, Von den Hoff JW. Matrigel, but not collagen I, maintains the differentiation capacity of muscle derived cells in vitro. Biomed Mater 2012; 7: 055004.
[43] Chen MH, Yang WK, Whang-Peng J, Lee LS, Huang TS. Differential inducibilities of GFAP expression, cytostasis and apoptosis in prima-

ry cultures of human astrocytic tumours. Apoptosis 1998; 3: 171-82.
[44] Chandel NS, Maltepe E, Goldwasser E, Mathieu CE, Simon MC, Schumacker PT. Mitochondrial reactive oxygen species trigger hypoxia-induced transcription. Proc Natl Acad Sci USA 1998; 95: 11715-20.
[45] Guzy RD, Hoyos B, Robin E, Chen H, Liu L, Mansfield KD, Simon MC, Hammerling U, Schumacker PT. Mitochondrial complex-III is required for hypoxia-induced ROS production and cellular oxygen sensing. Cell Metab 2005; 1: 401-8.
[46] Sullivan R, Paré GC, Frederiksen LJ, Semenza GL, Graham CH. Hypoxia-induced resistance to anticancer drugs is associated with decreased senescence and requires hypoxia-inducible factor-1 activity. Mol Cancer Ther 2008; 7: 1961-73.
[47] Gaspar N, Marshall L, Perryman L, Bax DA, Little SE, Viana-Pereira M, Sharp SY, Vassal G, Pearson AD, Reis RM, Hargrave D, Workman P, Jones C. MGMT-independent temozolomide resistance in pediatric glioblastoma cells associated with a PI3-kinase-mediated HOX/stem cell gene signature. Cancer Res 2010; 70: 9243-52.
[48] Nakada M, Kita D, Watanabe T, Hayashi Y, Teng L, Pyko IV. Aberrant Signaling Pathways in Glioma. Cancers 2011; 3: 3242-78.
[49] Rohlena J, Dong LF, Ralph SJ, Neuzil J. Anticancer drugs targeting the mitochondrial electron transport chain. Antioxid Redox Signal 2011; 15: 2951-74.
[50] Saraste M. Oxidative phosphorylation at the fin de siecle. Science 1999; 283: 1488-93.
[51] Wallace DC, Fan W, Procaccio V. Mitochondrial energetics and therapeutics. Annu Rev Pathol 2010; 5: 297-348.
[52] Bartek J, Lukas J. Mammalian G1- and S-phase checkpoints in response to DNA damage. Curr Opin Cell Biol 2001; 13: 738-47.
[53] Bartek J, Falck J, Lukas J. CHK2 kinase-a busy messenger. Nat Rev Mol Cell Biol 2001; 2: 877-86.
[54] Sarkar S, Mandal C, Sangwan R, Mandal C. Coupling G2/M arrest to the Wnt/β-catenin pathway restrains pancreatic adenocarcinoma. Endocr Relat Cancer 2014; 21: 113-25.
[55] Abraham RT. Cell cycle checkpoint signaling through the ATM and ATR kinases. Genes Dev 2001; 15: 2177-96.
[56] Shiloh Y. ATM and related protein kinases: safeguarding genome integrity. Nat Rev Cancer 2003; 3: 155-68.
[57] Bartek J, Lukas J. Chk1 and Chk2 kinases in checkpoint control and cancer. Cancer Cell 2003; 3: 421-29.
[58] Lukas C, Bartkova J, Latella L, Falck J, Mailand N, Schroeder T, Sehested M, Lukas J, Bartek J. DNA damage-activated kinase Chk2 is independent of proliferation or differentiation yet correlates with tissue biology. Cancer Res 2001; 61: 4990-3.
[59] Bunn HF, Poyton RO. Oxygen sensing and molecular adaptation to hypoxia. Physiol Rev 1996; 76: 839-85.
[60] Lluis JM, Buricchi F, Chiarugi P, Morales A, Fernandez-Checa JC. Dual role of mitochondrial reactive oxygen species in hypoxia signaling: activation of nuclear factor-{kappa}B via c-SRC and oxidant-dependent cell death. Cancer Res 2007; 67: 7368-77.

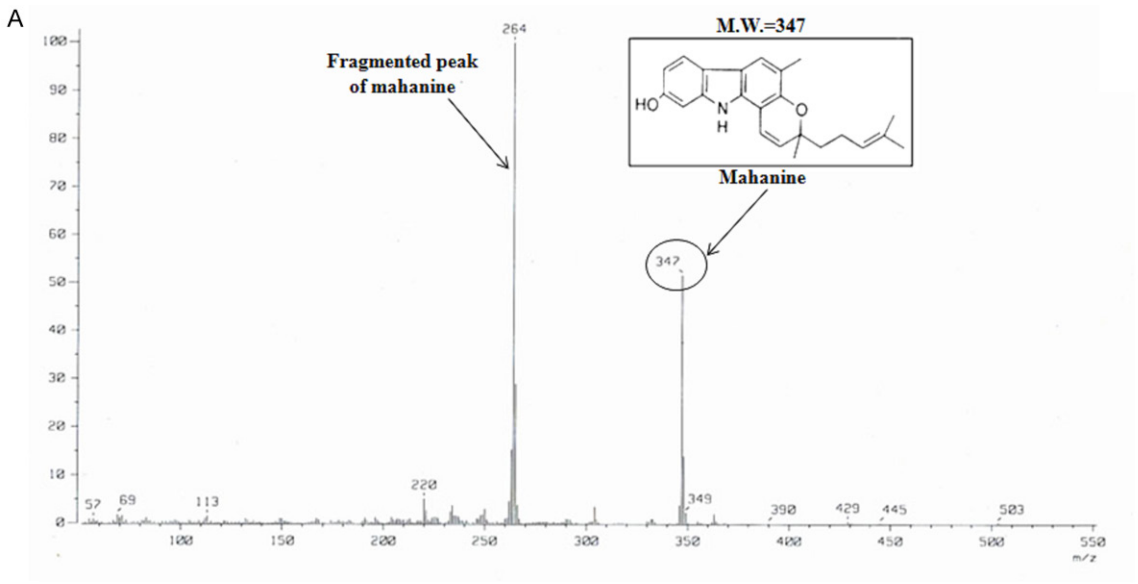

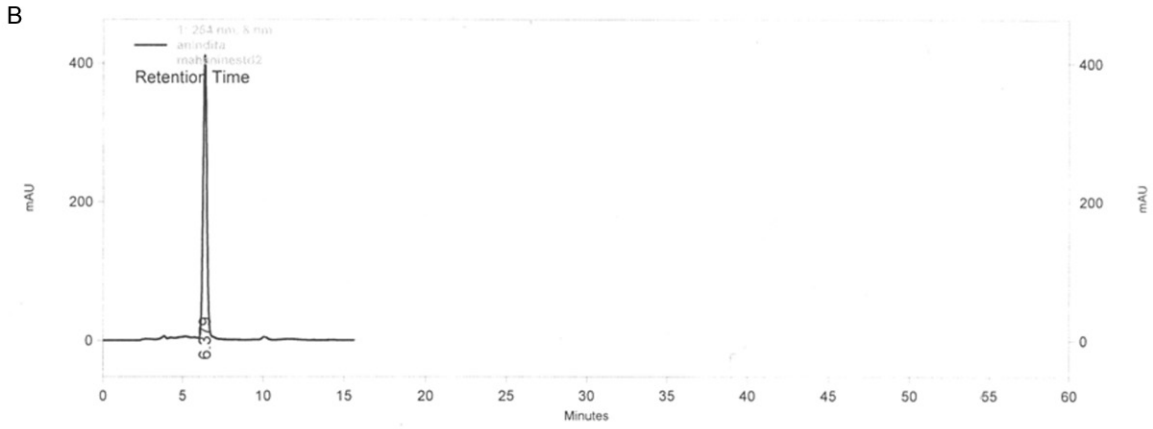

1: 254 nm, 8 nm

Pk #	Retention Time	Area	Area %	Height	Height %
1	6.379	64180	100.000	18624	100.000
Totals		64180	100.000	18624	100.000

Figure S1. A, B. FAB-MS and HPLC profile of mahanine and its purification status.

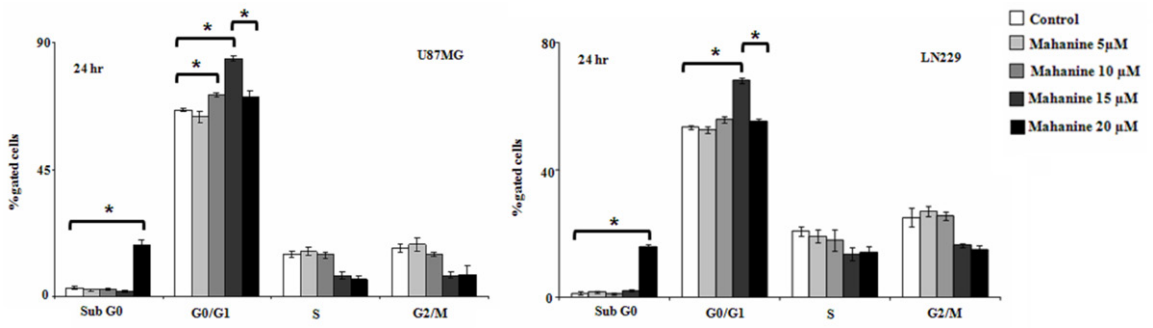

Figure S2. Mahanine induced G0/G1 phase cell cycle arrest in U87MG and LN229 cells in concentration dependent after 24 hr treatment. Each value is the mean ± SD of three independent experiments. *$P < 0.05$, significant difference between tow test groups.

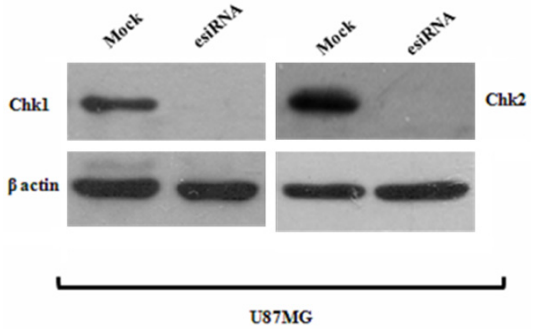

Figure S3. Confirmation of esiRNA-mediated knockdown of Chk1 and Chk2 in U87MG cells by Western blot analysis.

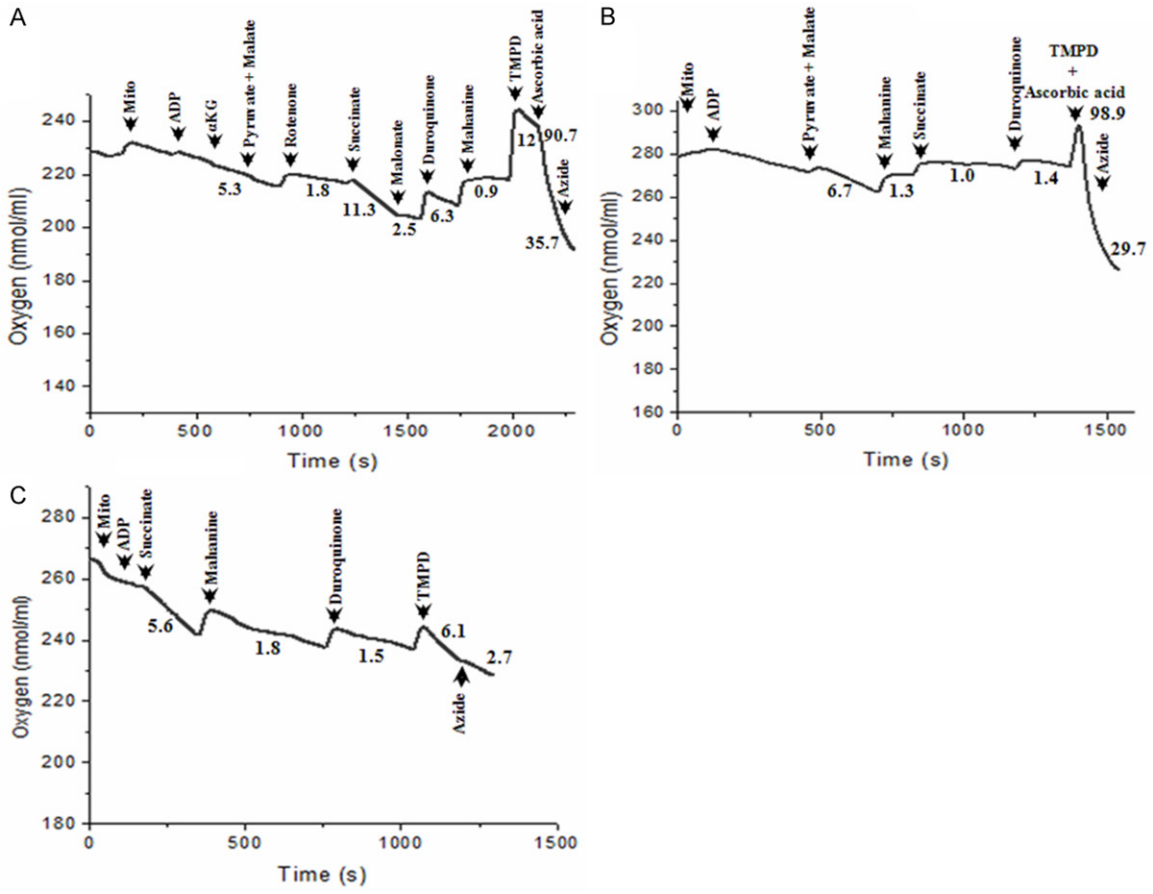

Figure S4. A. Establishment of complex-III inhibition by mahanine was confirmed by oxygraph analysis in isolated mitochondria from LN229 cell. Duroquinone-mediated enhanced mitochondrial respiration was significantly inhibited by mahanine. Mitochondria started respiration again after addition of substrate of complex-IV, TMPD alone or TMPD with ascorbic acid. B, C. Mahanine-mediated mitochondrial ETC inhibition could not initiate upon the addition of complex-II substrate (succinate) and complex-III substrate (duroquinone). Addition of TMPD again started the respiration which was inhibited by azide. All the numerical values are included in the plot is representing the rate of oxygen consumption by live isolated mitochondria (per mg).

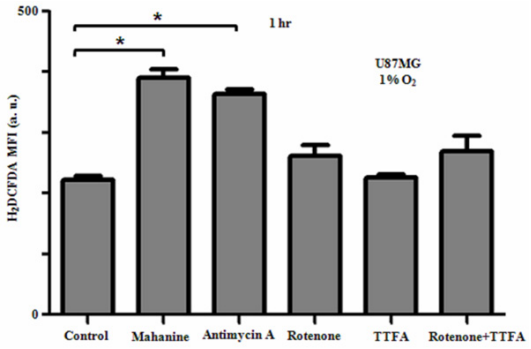

Figure S5. Only complex-III inhibitors [mahanine (20 μM) and antimycin A (15 μM)] were capable to induce enhance ROS in 1% hyoxia than rotenone (5 μM) and TTFA (5 μM) respectively complex-I and complex-II electron transfer inhibitor.

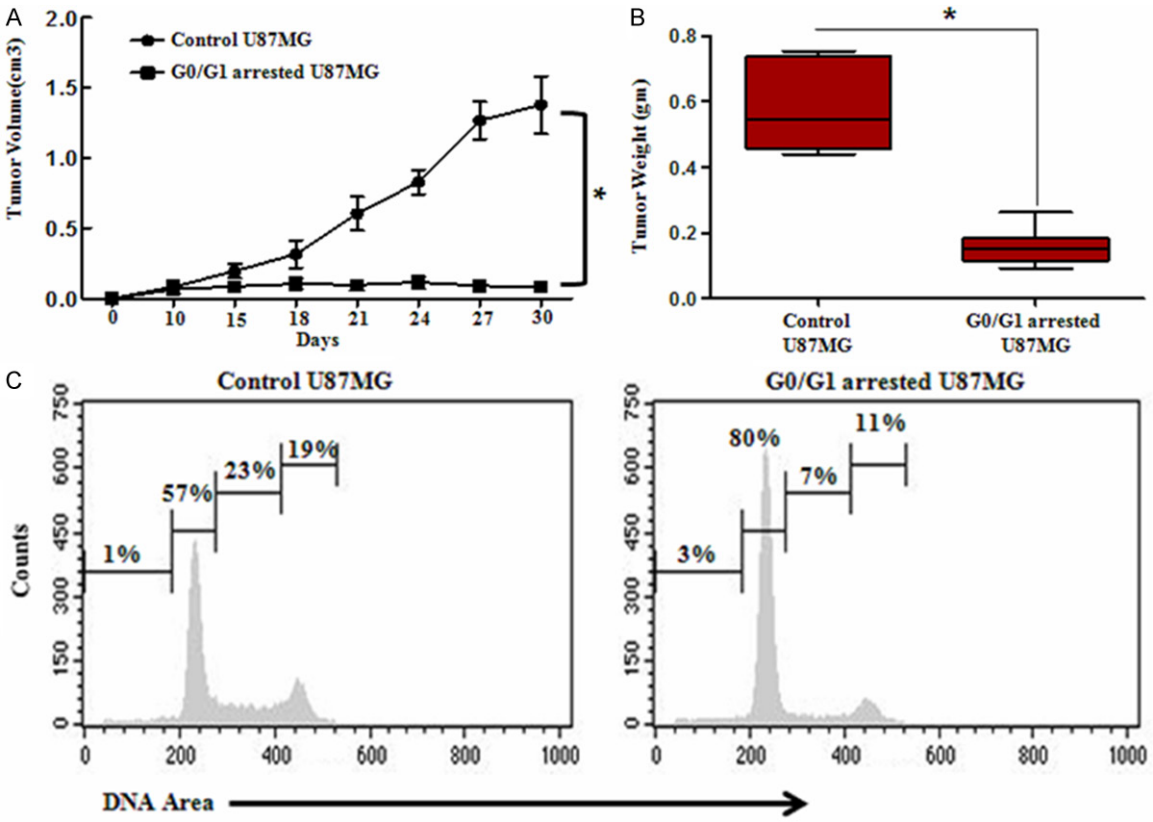

Figure S6. A. Graphical representation of progressive tumor volume between two groups of nude mice indicated that G0/G1 arrested cell had significantly reduced potential of tumor formation during 30 days time course. B. G0/G1 arrested U87MG cells produced very low weight tumor than U87MG cells by mahanine and control cells. Before the injection control and arrested cells were analyzed by PI staining and those population of arrested cells were injected where SubG0 cell population was ≤ 5%.